

Supplemental figures

BB0326 is responsible for the formation of periplasmic flagellar collar and the assembly of the stator complex in *Borrelia burgdorferi*

Hui Xu^{1#}, Jun He^{2#}, Jun Liu^{2*}, Md A. Motaleb^{1*}

¹ Department of Microbiology and Immunology, Brody School of Medicine, East Carolina University, Greenville, North Carolina, USA

² Department of Microbial Pathogenesis, Microbial Sciences Institute, Yale School of Medicine, New Haven, CT, USA

#Hui Xu and Jun He contributed equally.

*For correspondence: MD A. MOTALEB, E-mail: motalebm@ecu.edu, or JUN LIU, E-mail: jliu@yale.edu

Figure S1

1	MPDVKIIQF	KREILDNLSN	ERLSKESFGL	SMDVKLPEPG	ESIVPWIGED	LALDETDDDEL	DLNFMLDALE	NEDKLSYSDI
81	FNDNLPLSGS	NLRVDVDSEL	STLNNDFDVS	SSDSFENNID	KVLDDNSIDL	EIASKLDFDN	LINSPELSSE	ELINNQGNNN
161	FFEANNDSSV	LGDSNFLQSN	EFNIDDAVNG	KNQTDEQSEM	FVGDSLNLSA	DEDDFENVID	DFKFLEYDQN	ANFKRFEFKV
241	NYPLFLKHLN	SYPRNLRIAI	AEALTKENVS	RFKLEALIDL	VEKNKKRLKF	IAKFVGDIVG	RSIKLPVIYF	KAEEFSKLQQ
Transmembrane helix								
321	KLSYRVSRAL	LPLIKIASFF	VVLVLVSLYL	IVDVIFFYVA	SESKYKEGIE	SIYANKRDLA	KSIFRDAYYI	RPDDKWFINY
401	AKAFEDVRDF	DSAEKEYEEL	FTIEPFSKNS	TNRRRKKFNK	EGYISYASMK	IGLGEHSEAN	SILDEVISYD	LYDYDALVLK
PG-binding loop								
481	GDNYFKWAKT	NSNYKDSIN	SYTVVLSKYG	QKKEILFKLF	NAYIEANLDT	ESDNVNNFIK	SNEILDIDEV	VYTKYAKKLV
561	DKYISFVTYN	QRANNLAINL	NYLNGQTNLL	NKEFSDFKRN	DGRTIFKLDN	NVNMNSEIEY	ILRKILNKNP	NYDKALFESG
641	RYSYYIGDFK	KAEVYLLKAL	NSFRHKNSIE	DAGDKILAYK	ILADIYEKTR	DSLRSNIIG	LALSDYSFYK	KHNLIKGSKE
TPR repeat 1								
721	ISSIYEKQGD	ILRSLNDFKS	AISSYKLAIN	EGVDYPDVYY	KVGLLSYREN	NYDDALKYLF	KVESMAGFSS	SNEVLNTIAL
TPR repeat 2								
TPR repeat 3								
801	TLYKIGDFLA	SRSYYLRVMQ	NLELEKANVL	NFNPKENDYH	KTLLLKEIET	YNNLGVVEVM	ASFSSIRDTK	LFNSGVSNLS
881	ESAKIFDILN	RDEDMVKSVK	KDLASLNLRN	IFKNSFSKSN	VLFYENLSEK	L		

Figure S1. Amino acid sequence, membrane topology and the domain/motifs of BB0326 (931 aa., accession no. NP_212460.1). Transmembrane helix (aa 329-351) is predicted through TMHMM, potential peptidoglycan-binding site (aa 525-543) (see Fig. 1B) and TPR motifs (repeat 1: aa 736-750, repeat 2: 755-785, repeat 3: 792-820) were determined by analyzing the sequence using NCBI BLASTP.

Figure S2

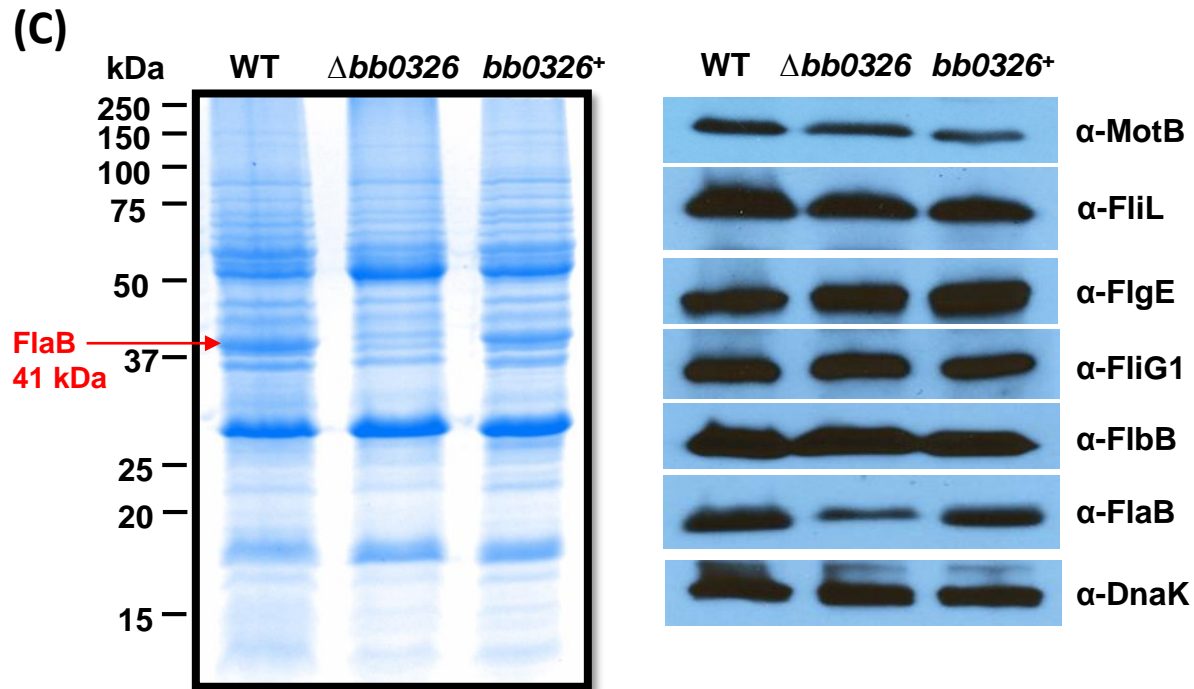
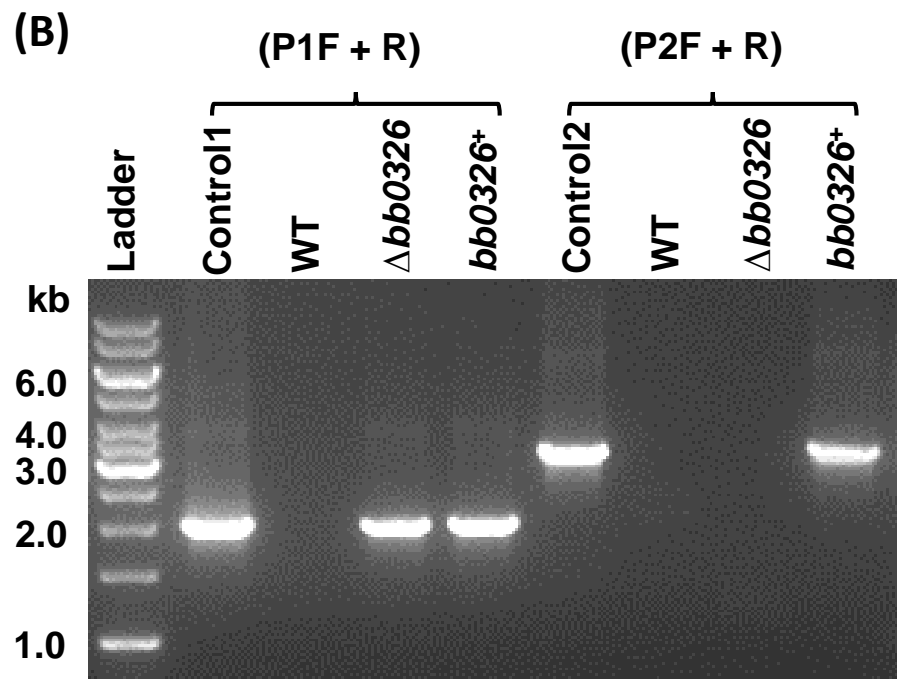
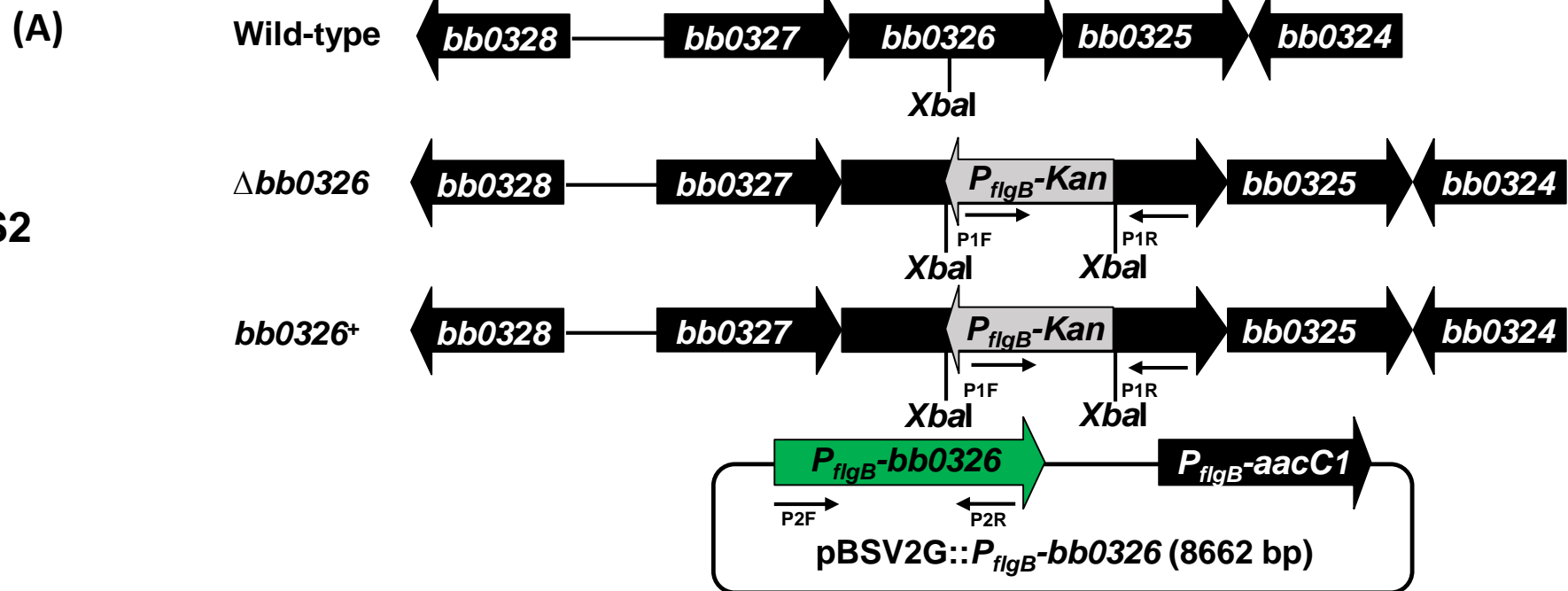


Figure S2. Inactivation and complementation of *bb0326*. (A) The *bb0326* gene is within an operon consisting of three genes (diagram is not to scale). The *bb0326* gene was inactivated by insertion of P_{flgB} -*Kan* cassette using allelic exchange mutagenesis in B31-A wild-type background. The *bb0326* mutant cells were complemented *in trans* using pBSV2G:: P_{flgB} -*bb0326* (8662 bp). (B) Confirmation of inactivation and complementation of $\Delta bb0326$ by PCR. (C) Effect of *bb0326* mutation on other flagellar protein syntheses were determined by Western blotting. Wild-type, $\Delta bb0326$, and *bb0326*⁺ cell lysates (10 μ g in each lane) were subjected to SDS-PAGE followed by coomassie staining. 41 kDa FlaB protein band is indicated by a red arrow (left). A gel ran parallelly was transferred to a PVDF membrane for immunoblot analysis (right). Immunoblots were performed with *B. burgdorferi* MotB, FliL, FlgE, FliG1, FliB, FlaB-specific antibodies. DnaK was used as a loading control.

Figure S3

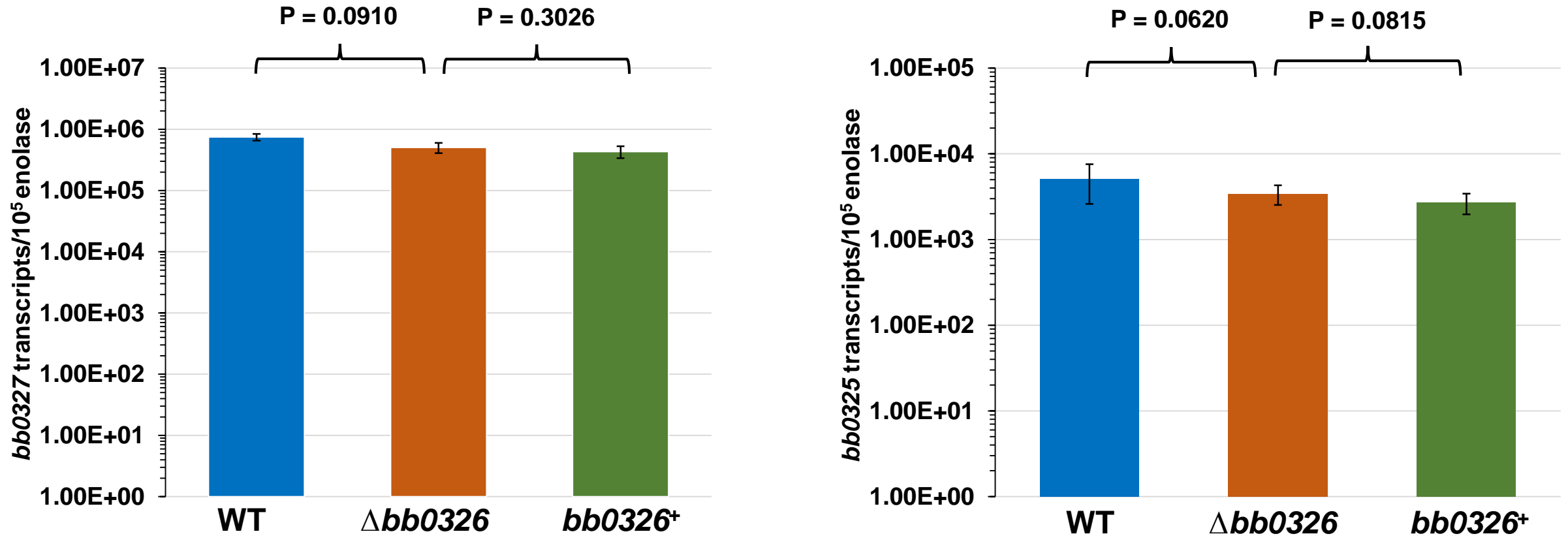


Figure S3. Expression of genes upstream and downstream of *bb0326* were not affected by the targeted mutagenesis of *bb0326*. Quantitative measurement of transcripts in the indicated spirochete clones by qRT-PCR. The relative transcript levels of *bb0327* (left), and *bb0325* (right) were determined in the wild-type, $\Delta bb0326$ and *bb0326*⁺ cells which were then compared with the expression of *B. burgdorferi enolase* gene. The bars represent mean \pm standard deviation of the mean from three independent samples. Statistical analysis was performed by using Student's *t*-test. P-values between samples are shown at the top. A P-value of <0.05 was evaluated as significantly different.

Figure S4

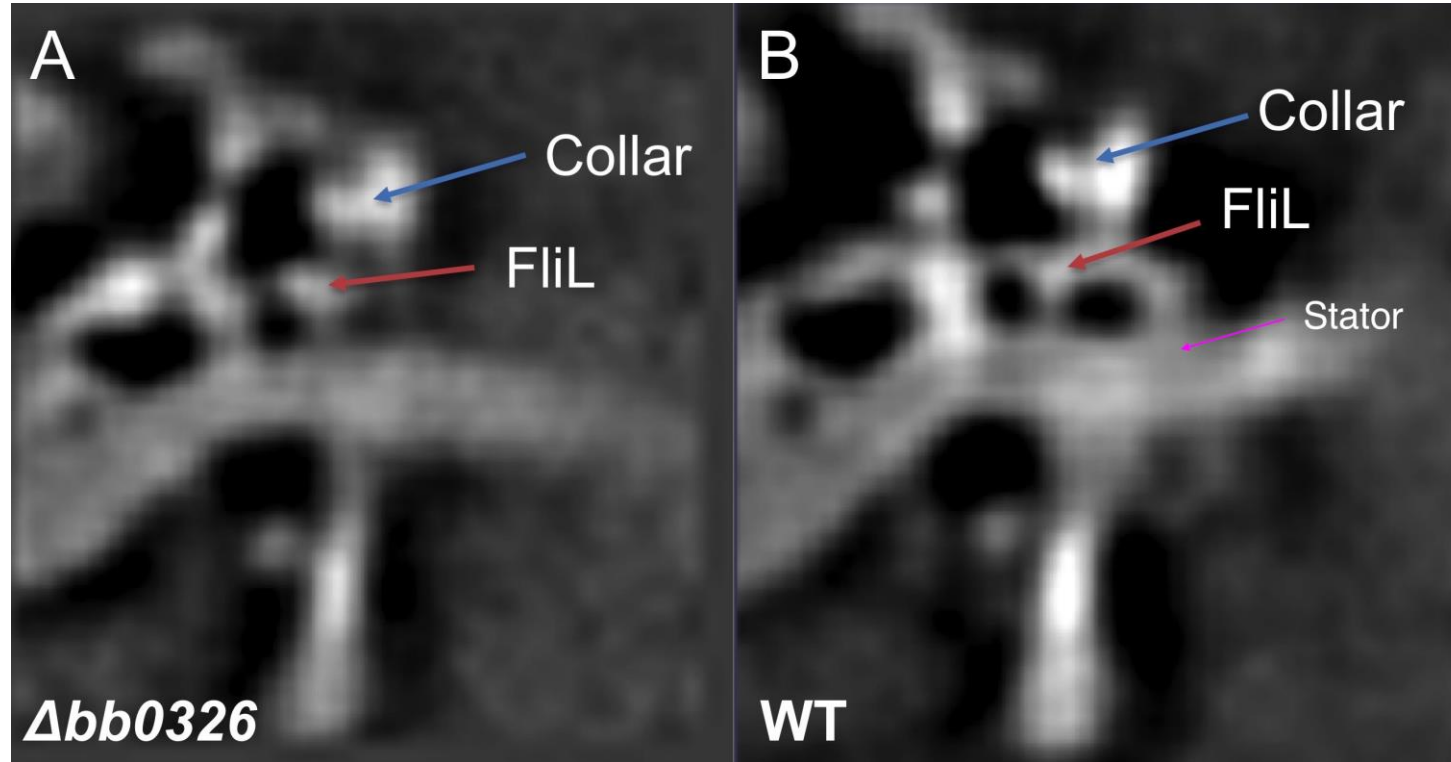


Figure S4. FliL assembly is not affected in the $\Delta bb0326/\Delta fliA$ mutant as determined by high-resolution cryo-ET. (A) An average structure of the flagellar motor from the $\Delta fliA$ mutant cells. **(B)** A similar average structure of the flagellar motor from the WT cells. Density around the FliL is shown to explicitly determine collar, FliL and stator structures.